AD-A066 699 CONSTRUCTION ENGINEERING RESEARCH LAB (ARMY) CHAMPAI--ETC F/G 13/1
THE PERFORMANCE OF AN EXPERIMENTAL SOLAR HEATING SYSTEM.(U)
FEB 79 D M JONCICH, D J LEVERENZ, D L JOHNSON

UNCLASSIFIED CERL-IR-E-144 NL

| OF |
AD
A066899

END
DATE
FILMED
5-79
DDC

construction engineering research laboratory

United States Army
Corps of Engineers
... Serving the Army
... Serving the Nation

INTERIM REPORT E-144
February 1979

LEVEL II

THE PERFORMANCE OF AN EXPERIMENTAL SOLAR HEATING SYSTEM

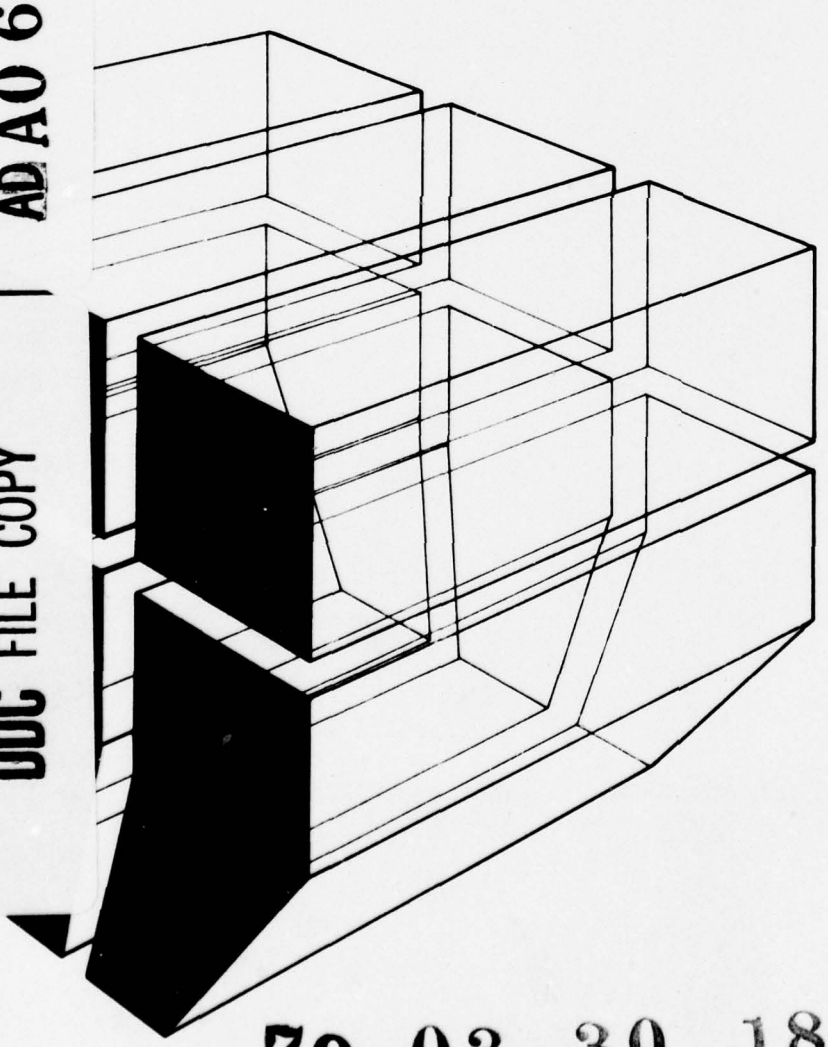

by
D.M. Joncich
D.J. Leverenz
D.L. Johnson

CERL

The contents of this report are not to be used for advertising, publication, or promotional purposes. Citation of trade names does not constitute an official indorsement or approval of the use of such commercial products. The findings of this report are not to be construed as an official Department of the Army position, unless so designated by other authorized documents.

DESTROY THIS REPORT WHEN IT IS NO LONGER NEEDED
DO NOT RETURN IT TO THE ORIGINATOR

UNCLASSIFIED

SECURITY CLASSIFICATION OF THIS PAGE (When Data Entered)

REPORT DOCUMENTATION PAGE	READ INSTRUCTIONS BEFORE COMPLETING FORM
1. REPORT NUMBER: CERL-IR-E-144	2. GOVT ACCESSION NO. / 3. RECIPIENT'S CATALOG NUMBER
4. TITLE (and Subtitle): THE PERFORMANCE OF AN EXPERIMENTAL SOLAR HEATING SYSTEM	5. TYPE OF REPORT & PERIOD COVERED: INTERIM rept.
	6. PERFORMING ORG. REPORT NUMBER
7. AUTHOR(s): D. M. Joncich, D. J. Leverenz, D. L. Johnson	8. CONTRACT OR GRANT NUMBER(s)
9. PERFORMING ORGANIZATION NAME AND ADDRESS: U. S. ARMY CONSTRUCTION ENGINEERING RESEARCH LABORATORY P. O. Box 4005, Champaign, IL 61820	10. PROGRAM ELEMENT, PROJECT, TASK AREA & WORK UNIT NUMBERS: 4A762731AT41-T6-021
11. CONTROLLING OFFICE NAME AND ADDRESS	12. REPORT DATE: February 1979
	13. NUMBER OF PAGES: ~~23~~ 26
14. MONITORING AGENCY NAME & ADDRESS (if different from Controlling Office)	15. SECURITY CLASS. (of this report): Unclassified
	15a. DECLASSIFICATION/DOWNGRADING SCHEDULE

16. DISTRIBUTION STATEMENT (of this Report)

Approved for public release; distribution unlimited.

17. DISTRIBUTION STATEMENT (of the abstract entered in Block 20, if different from Report)

18. SUPPLEMENTARY NOTES

Copies are obtainable from National Technical Information Service
Springfield, VA 22151

19. KEY WORDS (Continue on reverse side if necessary and identify by block number)

solar heating system
collector array
hot water storage tank

20. ABSTRACT (Continue on reverse side if necessary and identify by block number)

This report describes the performance of a residential-scale, completely instrumented solar heating system located at the U.S. Army Construction Engineering Research Laboratory (CERL), Champaign, IL. The investigation was made between January 1977 and April 1978. In addition, a daily profile of the performance of the system and its components is presented for a representative sunny winter day. An analysis of the solar system operation indicated that the collector array is by far the most inefficient component in the system for converting incident solar energy into useful heat. The solar system consists

CONT'

DD FORM 1 JAN 73 1473 EDITION OF 1 NOV 65 IS OBSOLETE

UNCLASSIFIED 405279

SECURITY CLASSIFICATION OF THIS PAGE (When Data Entered)

Block 20 continued.

of 20 m^2 (220 sq ft) of flat-plate, selective surface, singly glazed solar collectors and a 7.6 m^3 (2000 gal) equivalent hot water storage tank. The storage system supplies hot water for heating a 50 m^2 (540 sq ft) building used by CERL as office space. There is no domestic hot water in the building. Auxiliary energy is supplied by an electric, flow-through hot water heater. The results of this research are presented in terms of mean daily averages for each month during the heating season and include instantaneous solar radiation (horizontal and in the plane of the collector), useful heat acquired by the collector, useful heat delivered to the thermal storage tank, useful heat delivered to the heating load, thermal storage heat losses, and electrical energy supplied to the pumps.

FOREWORD

This work was performed for the Directorate of Military Construction, Office of the Chief of Engineers (OCE), under Project 4A762731AT41, "Design, Construction, and Operations and Maintenance Technology for Military Facilities"; Task T6, "Energy Systems"; Work Unit 021, "Solar Energy for Heating and Cooling of Buildings." Mr. S. Hiratsuka was the OCE Technical Monitor.

This study was performed by the Energy and Habitability Division (EH), U.S. Army Construction Engineering Research Laboratory (CERL). Mr. R. G. Donaghy is Chief of EH.

Appreciation is expressed to Mr. L. Randall Rippy, Nuclear Engineer, for his contribution in operating the system and collecting the data, and to Mr. George Shih, Mechanical Engineer, for his contribution to developing the original data analysis programs.

COL J. E. Hays is Commander and Director of CERL, and Dr. L. R. Shaffer is Technical Director.

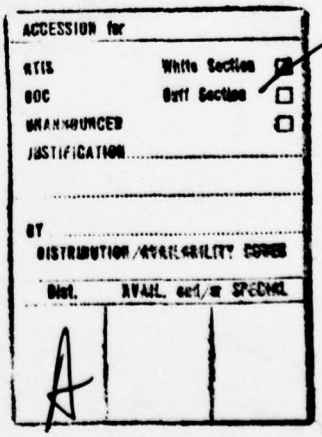

CONTENTS

TABLES

FIGURES

THE PERFORMANCE OF AN EXPERIMENTAL SOLAR HEATING SYSTEM

1 INTRODUCTION

Background

The technical feasibility of heating and cooling Army buildings using flat-plate solar collectors has been established both in theory and practice.[1] Although additional improvements in component and system design will be forthcoming, one can approach solar heating and cooling technology with full confidence that a practical, reliable system can be constructed. Because constructing solar systems requires little more skill than installing conventional heating and cooling systems, the widespread application of solar technology is primarily a question of economics; that is, can the Army save sufficient energy to offset the higher initial cost of the solar energy system?

To answer this question, the U.S. Army Construction Engineering Research Laboratory (CERL) has designed and constructed a residential-scale solar heating system and has monitored the actual performance of the system and its individual components.

Objective

The objective of this report is to analyze the actual performance of a residential solar heating system and its components for the 1977 and 1978 heating seasons. This research will provide Army designers with information about the energy losses to be expected from a solar energy system which uses flat-plate collectors. This research consisted of the following steps:

1. Determining the critical performance parameters for a solar heating system and designing an instrumentation system to collect data from which these performance parameters can be analyzed.

2. Procuring and installing a data-monitoring system on the solar system.

3. Collecting performance data.

4. Analyzing the collected data to determine the performance of the solar system in meeting the heating load of the building and the performance of the individual solar system components.

[1] D. C. Hittle, G. M. Walton, D. F. Holshouser, D. J. Leverenz, *Solar Energy for Heating and Cooling of Buildings*, Interim Report E-98/ADA035608 (U.S. Army Construction Engineering Research Laboratory [CERL], 1977).

Scope

This report describes only the solar energy system, the instrumentation package, and the actual performance of the flat-plate solar system and components used in this research. It does not compare this collected data with predictions for solar design tools developed by CERL or others.

Organization of Report

Chapter 2 describes the building and the solar energy system used in the research, and Chapter 3 describes the data collection instrumentation. Chapter 4 describes the performance of the solar system on a sunny winter day. Chapter 5 evaluates the solar system performance based on mean daily average for each month of the heating season and examines the performance of the major solar system components. Chapter 6 provides conclusions of the research.

Mode of Technology Transfer

The results of this study will be incorporated into an Engineer Technical Letter describing solar heating and cooling design procedures.

2 THE SOLAR TEST FACILITY AND SOLAR ENERGY SYSTEM

The CERL solar test facility is a 50 m^2 (540 sq ft) building which was retrofit with a solar heating system. Originally built to test a foam block construction concept, the structure is built of polystyrene blocks .15 m (6 in.) thick by .30 m (12 in.) high, and 2.4 to 3.0 m (8 to 10 ft) in length. Structural integrity is provided by poured concrete pillars .075 m (3 in.) in diameter, spaced on .6-m (2-ft) centers in the blocks. Because of the thickness of the polystyrene, the thermal losses of the structure are almost entirely the result of infiltration.

Figure 1 is a schematic of the solar system. The system contains an array of 12 singly glazed, selectively surfaced, flat-plate collectors which are facing south and tilted 30° from the horizontal. The collector pump circulates an inhibited water-glycol solution through the array so that each collector is subjected to a fluid flow of 3.97×10^{-5} m^3/sec (0.63 gpm) when the pump is active. The collector loop, which contains approximately .045 m^3 (12 gal) of fluid, is isolated from a pure water storage system by a single-pass, counterflow heat exchanger.

The storage tank is a 7.6-m^3 (2000-gal) precast concrete septic tank which has been foamed with .20 m (8 in.) of polyurethane insulation and partially

buried on the north side of the house. Two self-priming pumps (the storage pump and the load pump) circulate water from the tank. The storage pump connects the storage tank to the heat exchanger and is activated whenever the collector pump is energized. Together, these two pumps transfer energy from the collectors to the storage tank. The load pump delivers water from the tank to the heating coil whenever the room thermostat activates the heating system and the tank temperature exceeds 35°C (95°F).

Auxiliary energy is provided by a 12-kW electric in-line water heater when there is a demand for heat and the storage tank temperature has dropped below 35°C (95°F). The storage tank is bypassed when the auxiliary heater is used.

The control of energy flows within the house is entirely automatic. Solar energy collection begins whenever the collector plate is 5.6°C (10°F) warmer than the tank, and terminates when the collector is within 1.7°C (3°F) of the tank temperature. Heat distribution to the building is controlled by a room thermostat, in conjunction with an aquastat, a commercially available device which determines whether or not the tank temperature is above the 35°C (95°F) cut-off temperature. When solar energy is available, a demand for heat by the thermostat activates the load pump and distribution fan. As the tank temperature falls below 35°C (95°F), the position of the auto-valve changes and hot water from the resistance heater is delivered to the heating coil. In this case, the load pump and fan are still in operation.

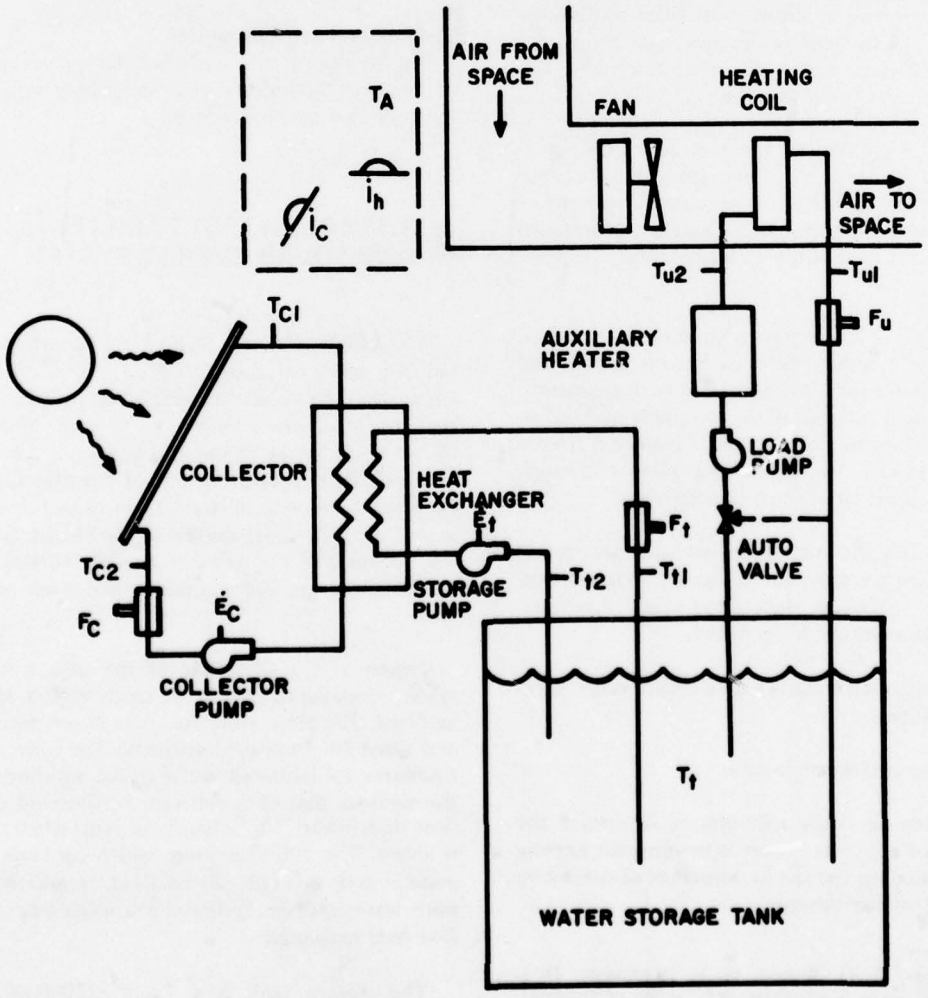

Figure 1. CERL solar facility (schematic).

3 PERFORMANCE PARAMETERS AND MEASUREMENT TECHNIQUE

Quantities Needed in a Solar Energy Performance Study

Estimating the performance of the solar heating system shown in Figure 1 requires a knowledge of the following quantities: the solar radiation, the heat flow between all major components, the electrical energy consumption of the pumps and auxiliary heater, the ambient temperature, and the storage tank temperature. The data points listed in Table 1 (also shown in Figure 1) were the basis for deriving the quantities given in Table 2.

The magnitude of solar radiation on the plane of the collector, I_C, was monitored to determine the total amount of solar energy available. In addition, the radiation on the horizontal plane was measured to determine the effect of tilting the collector on the amount of energy.

Heat was transferred between the major components by fluid flow. Consequently, the rate of heat transfer, $\dot{Q}$, was determined from

$$\dot{Q} = \varrho C_p F \Delta T \qquad \text{[Eq 1]}$$

where:

ϱ is the density of the fluid,
C_p is the specific heat of the fluid,
F is the volumetric fluid flow rate, and

ΔT is the temperature differential across the component

(Throughout this report, the notation $\dot{x} = \frac{dx}{dt}$ is employed *)

Measurements of the fluid flow rate and temperature differential associated with each major component were used in conjunction with Eq 1 to obtain the heat output of the collector, the heat input to the storage tank, and the heat delivered to the heating coil from the tank.

*Used for I, E, and Q.

Table 1
Data Points

Radiation	i_C	Radiation incident on the plane of the collector
	i_h	Radiation incident on the horizontal plane
Collector	T_{C1}	Collector inlet temperature
	T_{C2}	Collector outlet temperature
	F_C	Collector fluid flow rate
Tank	T_{t2}	Tank inlet temperature
	T_{t1}	Tank outlet temperature
	F_t	Tank fluid flow rate
	T_t	Tank temperature
Coil	T_{u2}	Heating coil inlet temperature
	T_{u1}	Heating coil outlet temperature
	F_u	Heating coil flow rate
Pumps	$\dot{E}_C$	Electrical energy consumption of collector pump
	$\dot{E}_C$	Electrical energy consumption of storage pump
Ambient	T_A	Ambient temperature

The amount of electrical energy consumed by the collector pump and storage pump was monitored to determine how much electrical energy was required to collect and store the solar energy. This measurement provides information about the cost of operating the system.

The ambient temperature was measured to determine how dependent the solar collector's thermal performance was on this quantity. This measurement, when combined with the collector and radiation measurements previously described, permits a comparison of the collector array performance with the model used by the National Bureau of Standards.[2]

Measurement Technique

The instantaneous values of the data points listed in Table 1 were recorded each hour on tape, using a 40-channel data acquisition system in combination with a magnetic tape recorder. The Appendix lists the sensors and instrumentation used. Electronic analog integrators were employed to perform the integrations for the quantities listed in Table 2. The amount of heat transfer between major components was obtained by using electronic multipliers to obtain the $F\Delta T$ products before the integrations were performed. All integrations were performed for 1-hour intervals, and the values were recorded each hour simultaneously with the instantaneous values listed in Table 1.

A special feature of the measurement technique used for the CERL Solar Facility is the high accuracy of the method used to obtain the fraction of the load supplied by the solar system. Heat from both the auxiliary source and the solar system was supplied in the form of hot water to the same heating coil; therefore, it was possible to use the same sensors and signal-conditioning instrumentation to obtain the $F\Delta T$ products corresponding to heat from both sources. Two integrators were used to obtain this $F\Delta T$ product: one integrator, activated only when the flow to the coil was from the solar tank, provided a value for the useful heat supplied by the solar system; the other integrator, activated at all times, was used to obtain a value for the total heat supplied to the heating coil.

Since the fraction of the load supplied by the solar system is the ratio of these two quantities, many of the instrument errors cancel when this ratio is calculated. The Appendix includes an illustration of this method. Table A1 of the Appendix is a complete listing of instrument accuracies. A magnification of instrument errors, a problem that commonly occurs when subtracting two large numbers, was experienced when calculating energy losses from the heat exchanger and tank. These losses are the difference in the input and output energy transfer determined from Eq 1. Using the typical value of 2°C (3.6°F) from the temperature difference in Eq 1 and the instrument accuracies given in the Appendix, the total estimate of error for these two energy measurements was found to be ±5.5 percent. Although this accuracy is satisfactory for evaluating the overall system performance, the size of this error makes it difficult to evaluate the energy losses of the heat exchanger and tank (the magnitude of which is typically 5 to 15 percent of the energy transferred).

[2] J.S. Hill and T. Kusuda, *Methods of Testing for Rating Solar Collectors Based on Thermal Performance*, NBSIR-74-685 (National Bureau of Standards, 1974).

4 THE SOLAR SYSTEM PERFORMANCE ON A SUNNY WINTER DAY

Figure 2 illustrates the performance of the solar system on February 5, 1977. Because the sun was shining all day and the ambient temperature was relatively low [-7°C (20°)], the system response during this time was representative of wintertime operation on a sunny day (No energy was withdrawn from the solar tank during the time pictured on the figure.) The circles show the instantaneous values of the solar radiation incident upon the collector array for each hour in Figure 2 and indicate the magnitude of the instantaneous power available to the collector. The amount of energy collected during each hour is shown by a pair of squares separated by a dashed line. Using only these two quantities, it is possible to calculate the system's average efficiency. For example, the incident solar power was roughly constant at a value of 18 kW from hour 12 to 13, whereas the collector yielded 5.8 kWh of energy for this interval. Hence, the efficiency for this time interval is approximately 32 percent. The figure shows that the efficiency is not constant throughout the day. On the contrary, the figure indicates a very low efficiency during the early morning and late afternoon hours, with no collection occurring before 0900 or after 1600 hours, even though an appreciable amount of solar radiation is available. This characteristic behavior occurs because a threshold of radiation must be reached to offset thermal losses to the ambient air before the energy is collected. The major energy collection occurs over a 5-hour period (1000 to 1500 hours).

Figure 2 also shows the amount of electrical energy that the pumps consume each hour in collecting the solar energy. The ratio of this quantity to the energy collected remains at a value of approximately 10 percent throughout the day. The tank temperature shown in the figure indicates the occurrence of energy collec-

tion in terms of a temperature increase. The relation between the tank temperature and tank energy is given by

$$\Delta Q = \rho V C_p \Delta T \qquad \text{[Eq 2]}$$

where V is the tank volume.

The temperature increase of 4.4°C (7.9°F) for this day corresponds to an increase in tank energy of 37 kWh compared to a value of only 25 kWh for the energy collected. This discrepancy arises from the fact that the tank temperature sensor is a "point" probe, which measures the water temperature in the immediate vicinity of the probe but does not provide the average tank temperature. When a point probe is used to measure tank temperature, it is necessary to insure that the tank has equilibrated before this value can be used in Eq 2 to obtain the tank's energy change.

Finally, Figure 2 summarizes the system performance for hour 1300 by listing the actual values of the data points shown in Figure 1.

5 EVALUATION OF SOLAR SYSTEM PERFORMANCE

Daily Averages for 1977-78 Heating Season

Table 3 lists in SI units the data obtained for the solar system performance during the 1977 and 1978 heating seasons. Table 4 lists these data in British units. The data are presented in the form of daily averages for each month as defined by Eq 3:

$$X = \frac{\sum_{i=1}^{n} Xi}{n} \qquad \text{[Eq 3]}$$

where: n is the number of days that data were collected during the month,

X_i is the total value obtained for the i^{th} day, and

X is the daily average of the quantity for the month.

The data are presented in this form because it allows representative values to be determined for each month, even though data were unavailable for several days of that month because of equipment failure. Tables 3 and 4 list the number of days of data collection for each month.

The third column in Tables 3 and 4 gives the daily average of the solar energy incident per unit area on both the collector plane and the horizontal plane. This is followed by a column listing the daily average of the collector's heat output. The columns under the heading "Tank" give the daily averages of the heat input to the tank, the heat lost by the tank to the surroundings, the useful heat delivered from the tank to the heating coil, and the fraction of the heating load

Table 2
Quantities Obtained From Data Points

Incident solar energy per unit area on collector plane	$I_C = \int i_C \, dt$
Incident solar energy on collector (A_C = area of collector array)	$I = I_C A_C$
Incident solar energy per unit area on horizontal plane	$I_h = \int i_h \, dt$
Collector heat output rate	$\dot{Q}_{out} = C_p \rho F_C (T_{C2} - T_{C1})$
Collector heat output	$Q_{out} = \int \dot{Q}_{out} \, dt$
Tank heat input	$Q_{in} = C_p \rho \int F_t (T_{t2} - T_{t1}) \, dt$
Useful heat supplied by solar system to coil *integrated only when coil is supplied by tank	$Q_{used} = C_p \rho \int^{*} F_u (T_{u2} - T_{u1}) \, dt$
Total heat supplied to coil (by solar and auxiliary)	$Load = C_p \rho \int F_u (T_{u2} - T_{u1}) \, dt$
Electrical energy consumed by pumps to collect and store solar energy	$E = \int (\dot{E}_C + \dot{E}_t) \, dt$

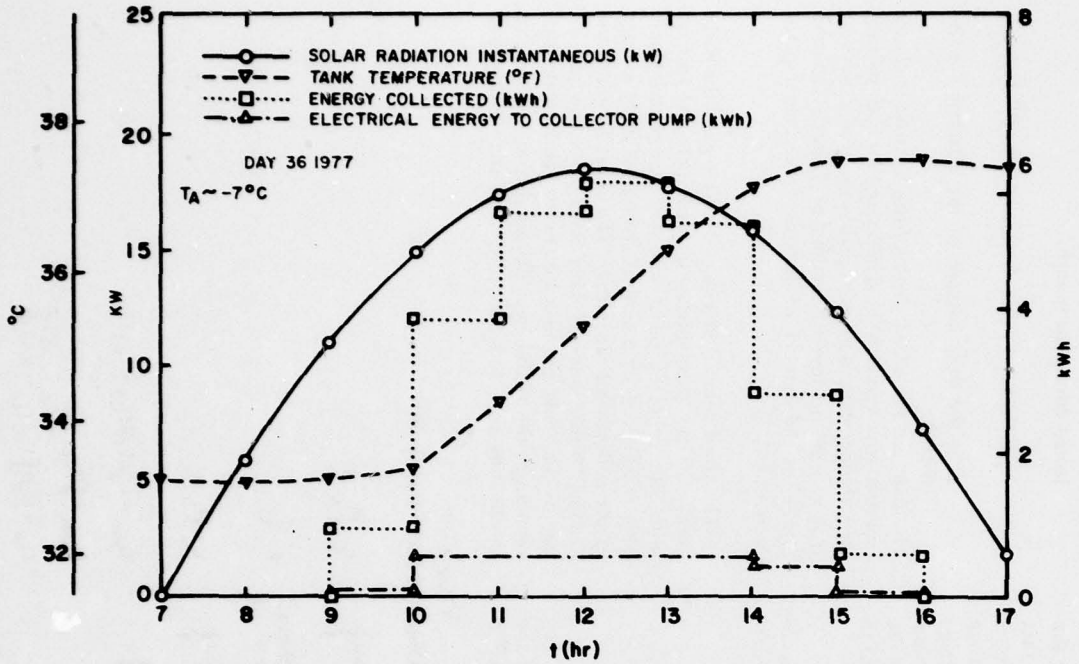

Data at hour 13:00 for
Day 36, 1977

T_{C1}	40.4°C (105°F)	T_H	36.2°C (97°F)	T_t	36.3°C (97°F)
T_{C2}	47.1°C (117°F)	T_{t2}	37.9°C (100°F)	T_A	-6.3°C (21°F)
Q_{out}	5.86 kWh (2.0×10^4 Btu)	$\dot{I}_C$	17.4 kW (5.9×10^4 Btu/hr)	E	0.56 kWh (1.91×10^3 Btu)
Q_{in}	5.45 kWh (1.86×10^4 Btu)	$\dot{I}_h$	11.9 kW (4.06×10^4 Btu/hr)		

Figure 2. Typical sunny winter day solar system performance.

supplied by the solar system. The last column gives the average daily electrical consumption of the pumps used to collect and store the solar energy.

Overall System Performance

The magnitudes of the energy transfer between major system components listed in Tables 3 and 4 (denoted by Q_{out}, Q_{in}, and Q_{used}) depend on the size of the solar collector array. Consequently, a more universal measure of the solar system performance is obtained by dividing the energy transfer by the area of the collector array. This facilitates the extrapolation of these results to other systems. Tables 5 and 6 contain the results, in SI and British units, respectively, of using this scaling procedure. To insure that a representative value of overall system performance was obtained, the values in the tables are from months for which sufficient data were available.

To measure the solar system's overall efficiency, the values for the energy transfer between major components have been divided by the total incident solar energy (see Table 7). This table indicates that the collector, which has an efficiency of nearly 25 percent, is by far the most inefficient component. The fraction of the incident solar energy delivered to the heating coil ranges from 19.5 to 25.8 percent.

The amount of solar radiation striking the surface of the collector depends on the collector's tilt angle. Table 8 shows the effect of the collector inclination on the incident solar energy's magnitude for the CERL array (30° tilt). This table lists the ratio of the solar energy incident upon the collector plane to the solar energy incident upon the horizontal plane. The effect of the inclination ranges from an incident energy increase of 30 percent for the month of February 1977, to a decrease of 18 percent for April 1978.

Component Performance

Heat Exchanger

The heat exchanger was used to isolate the collector loop containing an anti-freeze solution from the water in the tank. The daily averages of the heat output of the collectors and the heat input to the tank given in Tables 3 and 4 were used to calculate the heat exchanger's efficiency. The results, given in Table 9, reveal an average efficiency of 94 ± 4 percent. The variation in the values listed in Table 9 is probably the result of the inherent problem of taking small differences between large measured values (see Measurement Technique section).

In addition to the direct heat loss to the ambient air, another detrimental effect arises from using the heat exchanger. The fact that the heat exchanger effectiveness is less than 1 results in an increase in the collector operating temperature and a resultant decrease in collector efficiency. An examination of the typical values of the collector inlet and tank outlet temperatures revealed that an increase in collector operating temperature of approximately 4°C (7.2°F) was associated with using the heat exchanger. Since a calculation based on the collector performance curve (see *Collectors* section) gave a value of roughly 0.5 percent/C

Table 3
Performance of CERL Solar Test Facility, 1977–78
Daily Averages for Each Month in SI Units

Month and Year	Days Data Collected	Solar Radiation (kWh/m²)		Collector		Tank			Elec. Power
		Coll. Plane	Horiz. Plane	Q_{out} (kWh)	Q_{in} (kWh)	Q_{lost} (kWh)	Q_{used} (kWh)	$\frac{Q_{used}}{Load}$	E (kWh)
Jan 1977	9	2.30	2.07	6.7	6.4	1.4	5.3	7.0%	0.82
Feb 1977	27	3.30	2.53	18.1	17.0	1.5	16.5	36.4%	1.87
Mar 1977	28	3.50	3.20	17.8	16.4	2.3	14.1	44.2%	2.02
Apr 1977	24	3.01	3.20	17.4	16.9	0.4	13.5	71.0%	1.72
May 1977	4	3.10	3.62	25.6	23.0		0.4	100.0%	2.57
Jan 1978	30	2.36	1.96	*	10.3	0.4	11.1	9.5%	1.01
Feb 1978	25	3.16	2.97	*	16.6	0.9	16.2	16.6%	1.53
Mar 1978	28	2.97	3.13	*	20.3	1.4	15.9	24.4%	1.84
Apr 1978	5	3.37	4.11	*	31.7	–	22.0	80.0%	2.82

*Data unavailable due to failure of collector inlet temperature measurement.

Table 4
Performance of CERL Solar Test Facility, 1977–1978
Daily Averages for Each Month in British Units

Month and Year	Days Data Collected	Solar Radiation (Btu/sq ft) Coll. Plane	Solar Radiation (Btu/sq ft) Horiz. Plane	Collector Q_{out} (10^3 Btu)	Collector Q_{in} (10^3 Btu)	Tank Q_{lost} (10^3 Btu)	Tank Q_{used} (10^3 Btu)	Tank $\frac{Q_{used}}{Load}$	Elec. Power E (10^3 Btu)
Jan 1977	9	730	660	22.9	21.8	4.8	18.1	7.0%	2.8
Feb 1977	27	1050	800	61.8	58.0	5.1	56.3	36.4%	6.4
Mar 1977	28	1110	1010	60.7	56.0	7.8	48.1	44.2%	6.9
Apr 1977	24	950	1010	59.4	57.7	1.4	46.1	71.0%	5.9
May 1977	4	980	1150	87.4	78.5	-	1.4	100.0%	8.8
Jan 1978	30	750	620	*	35.2	1.4	37.9	9.5%	3.5
Feb 1978	25	1000	940	*	56.7	3.1	55.3	16.6%	5.2
Mar 1978	28	950	990	*	69.3	4.8	54.3	24.4%	6.4
Apr 1978	5	1070	1300	*	108.2	-	75.1	80.0%	9.6

*Data unavailable due to failure of collector inlet temperature measurement.

Table 5
Performance of System Scaled by Area of Collector Array
SI Units

Month and Year	Collector $\frac{Q_{out}}{A_C}$ (kWh/m^2)	Tank $\frac{Q_{in}}{A_C}$ (kWh/m^2)	Tank $\frac{Q_{used}}{A_C}$ (kWh/m^2)
Feb 1977	0.87	0.82	0.80
Mar 1977	0.86	0.79	0.68
Apr 1977	0.84	0.82	0.65
Jan 1978	-	0.50	0.54
Feb 1978	-	0.80	0.78
Mar 1978	-	0.98	0.77

Table 6
Performance of System Scaled by Area of Collector Array
British Units

Month and Year	Collector $\frac{Q_{out}}{A_C}$ (Btu/sq ft)	Tank $\frac{Q_{in}}{A_C}$ (Btu/sq ft)	Tank $\frac{Q_{used}}{A_C}$ (Btu/sq ft)
Feb 1977	276	260	254
Mar 1977	273	250	216
Apr 1977	267	260	206
Jan 1978	–	159	172
Feb 1978	–	254	247
Mar 1978	–	311	244

Table 7
Performance of System Expressed in Terms of Incident Solar Energy

Month and Year	Collector $\frac{Q_{out}}{I}$	Tank $\frac{Q_{in}}{I}$	Tank $\frac{Q_{used}}{I}$
Feb 1977	26.4%	24.9%	24.1%
Mar 1977	24.6%	22.6%	19.5%
Apr 1977	27.9%	27.1%	21.6%
Jan 1978	–	21.1%	22.7%
Feb 1978	–	25.4%	24.7%
Mar 1978	–	33.0%	25.8%

Table 8
Effect of Collector Inclination on Incident Solar Energy

Month	$\frac{I_{coll.}}{I_{horiz.}}$ 1977	$\frac{I_{coll.}}{I_{horiz.}}$ 1978
Jan	1.11	1.20
Feb	1.30	1.06
Mar	1.09	0.95
Apr	0.94	0.82
May	0.86	–

Table 9

Performance of Heat Exchanger

Month and Year	$\frac{Q_{in-tank}}{Q_{out-coll.}}$
Jan 1977	.95
Feb 1977	.94
Mar 1977	.92
Apr 1977	.97
May 1977	.90

Table 10
Electrical Energy Consumption By Pumps

Month	$\frac{E}{Q_{in-tank}}$ 1977	1978
Jan	12.8%	9.8%
Feb	11.0%	9.2%
Mar	12.3%	9.1%
Apr	10.2%	8.9%
May	11.2%	–

for the decreased collector efficiency per unit temperature increase, the use of the heat exchanger causes a 2 percent decrease in the collector's heat output. A 2 percent loss, when calculated for this particular collector-heat exchanger combination, indicates that the heat exchanger was sized properly.

Pumps

To obtain a proper perspective of the daily average electrical energy consumption of the pumps that collect and store the solar energy, this quantity should be compared to the amount of energy delivered to the tank in return for this expenditure. Table 10 lists the ratio of the electrical energy consumption to the tank heat input for each month. Since the values range from 8.9 to 12.8 percent, the results indicate that the solar system delivers roughly 9 units of energy to the tank for each unit of electrical energy consumed. These values could probably be improved, since the pump sizes used for this solar system are somewhat larger than necessary for this collector array.

Storage Tank

The storage tank losses given in Tables 3 and 4 were calculated using an energy-balance technique. The energy lost was taken to be the difference between the next heat input to the tank (the heat input to the tank minus the heat output to the coil) and the change in tank energy indicated by the change in tank temperature. This method is as shown in Eq 4.

$$Q_{lost} = (Q_{in} - Q_{used}) - \Delta Q_t(T) \quad \text{[Eq 4]}$$

where: Q_{in} is the daily average heat input to the tank,

Q_{used} is the daily average useful heat delivered to the coil, and

$\Delta Q_t(T)$ is the change in tank energy indicated by the temperature.

The change in tank energy was calculated using the expression for heat capacity given in Eq 2.

To evaluate the impact of the storage tank losses on solar system performance, the daily average storage tank losses should be compared to the daily average heat input to the tank. The ratio of these two quantities then gives the fraction of the energy lost by the tank and indicates the tank's heat retention ability for this application. The large variation in the daily average tank losses given in Tables 3 and 4 is thought to be the result of the difficulties in determining $\Delta Q_t(T)$. Consequently, these quantities were averaged over the entire year (see Table 11) in an effort to reduce the error produced by this term in Eq 4. The fraction of the heat input to the tank that is lost to the ambient air is given there as a 9.2 percent for 1977 and 5.7 percent for 1978. Since the conditions affecting tank loss were nearly constant for 1977 and 1978, these values are thought to reflect the difficulties in measuring the differences in two large numbers (i.e., $Q_{in} - Q_{used}$ in Eq 4). A calculation of the fractional tank losses , based on the handbook value of the insulation resistance and other known tank characteristics, yielded an average value of 15 percent for 1977 and 14 percent for 1978. The relatively high tank losses calculated for this solar system are the result of the

Table 11

Thermal Storage Losses

Year	Daily Average Q_{lost} (kWh)	Daily Average $Q_{in-tank}$ (kWh)	Ratio $\frac{Q_{lost}}{Q_{in-tank}}$
1977	1.44	15.7	9.2%
1978	0.89	15.6	5.7%

high ratio of tank volume to collector array area [.38 m^3/m^2 (9 gal/sq ft)] used for this system. The high losses are compensated by the fact that the additional energy storage occurring in the summer is used in the fall months.

Collectors

The daily average efficiency of the collectors (Table 7) was found to be only about 25 percent. Comparing the collector's performance with that of the other components listed in Tables 3 and 4 reveals that it is by far the most inefficient component. Consequently, its performance was investigated in detail to identify the sources responsible for the loss of collector efficiency. To accomplish this task, a procedure consistent with the one defined by the National Bureau of Standards (NBS)[3] was used. In the procedure, the instantaneous efficiency, η, is plotted versus the fluid parameter, F. These quantities are defined by Eqs 5 and 6.

$$\eta = \frac{Q_{out}}{I} \qquad \text{[Eq 5]}$$

$$F = \frac{\bar{T}_F - T_A}{I/A_C} \qquad \text{[Eq 6]}$$

where: Q_{out} is the energy output of the collector,

I is the incident solar energy,

$\bar{T}_F$ is the average fluid temperature,

T_A is the ambient temperature, and

A_C is the area of the collector absorber plate.

In the NBS procedure, the measurements are taken under quasi-steady conditions for a 15-minute interval; here, however, the available data were collected under ambient conditions at 1-hour intervals.

Figure 3 shows the results of applying these procedures for the data points collected during the 1977–78 heating seasons. Also shown are the test results for a single collector performed in March 1976 by Desert Sunshine Exposure Test Inc., Phoenix, AZ.

The results shown in Figure 3 can be interpreted by using the following model. Under steady-state conditions, the energy output of the collector is simply the difference between the energy absorbed by the collector plate and the energy lost by the conduction and convection of energy to the surroundings. This relationship is expressed in Eq 7.

$$Q_{out} = Q_{abs} - Q_{con} \qquad \text{[Eq 7]}$$

where: Q_{out} is the energy output of the collector,

Q_{abs} is the energy absorbed by the collector plate, and

Q_{con} is the energy lost by conduction.

The energy absorbed by the collector can be expressed as a fraction, η_o, of the incident solar energy (I), as given in Eq 8.

$$Q_{abs} = \eta_o I. \qquad \text{[Eq 8]}$$

The fraction η_o, takes into account the solar transmittance of the glass and the absortivity of the selectively coated plate. Although these quantities depend on the angle of the radiation's incidence, this effect is neglected in this sample model.

The rate of energy loss by conduction and convection will be roughly proportional to the total collector area and the temperature difference between the collector (T_C) and the ambient air (T_A). This defines an effective U-value (U_{eff}) as given by:

$$\dot{Q}_{con} = U_{eff} A_T (T_C - T_A) \qquad \text{[Eq 9]}$$

where: A_T is the total collector area, including the front, back, and side surfaces.

In this simple model, various complicating factors associated with the convective heat losses (such as dependencies on temperature and air speed) are neglected. Radiation losses, which amount to approximately 5 percent under normal operating conditions, are also neglected. In this method, the collector temperature is the average fluid temperature, $\bar{T}_F$.

Using Eqs 5, 6, 7, 8, and 9, the instantaneous efficiency is given in this simple model by Eq 10.

$$\eta = \eta_o - \frac{[U_{eff} A_T]F}{A_C} \qquad \text{[Eq 10]}$$

Hence, this simple model predicts that the plot of η vs. F will be a straight line with negative slope. The behavior observed in the single-collector test shown in Figure 3 clearly agrees with the predictions of the model. This plot provides a convenient method for accounting for collector efficiency losses when operating condi-

[3] J. S. Hill and T. Kusuda, *Methods of Testing for Rating Solar Collectors Based on Thermal Performance*, NBSIR–74–635 (National Bureau of Standards, 1974).

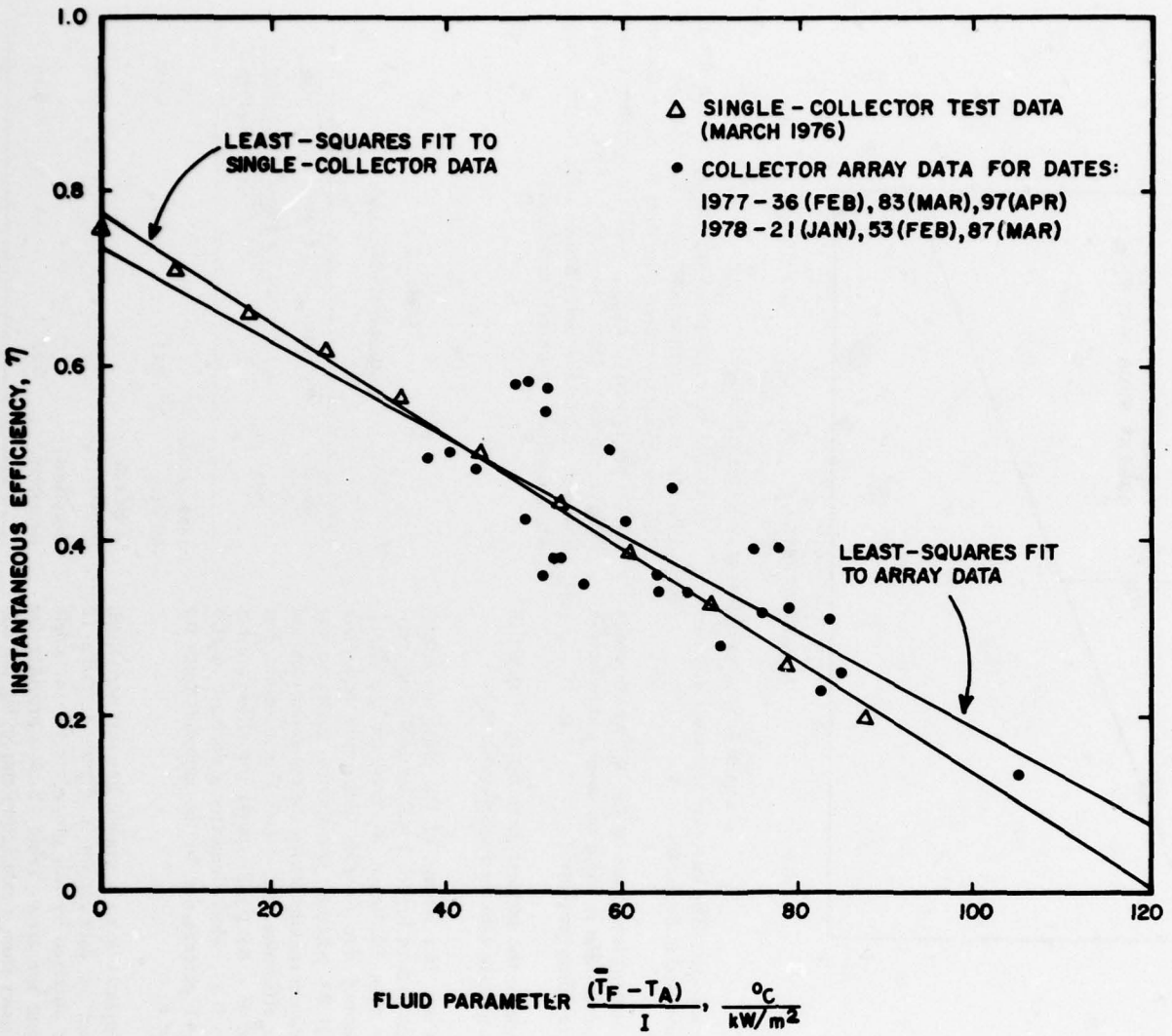

Figure 3. Collector performance.

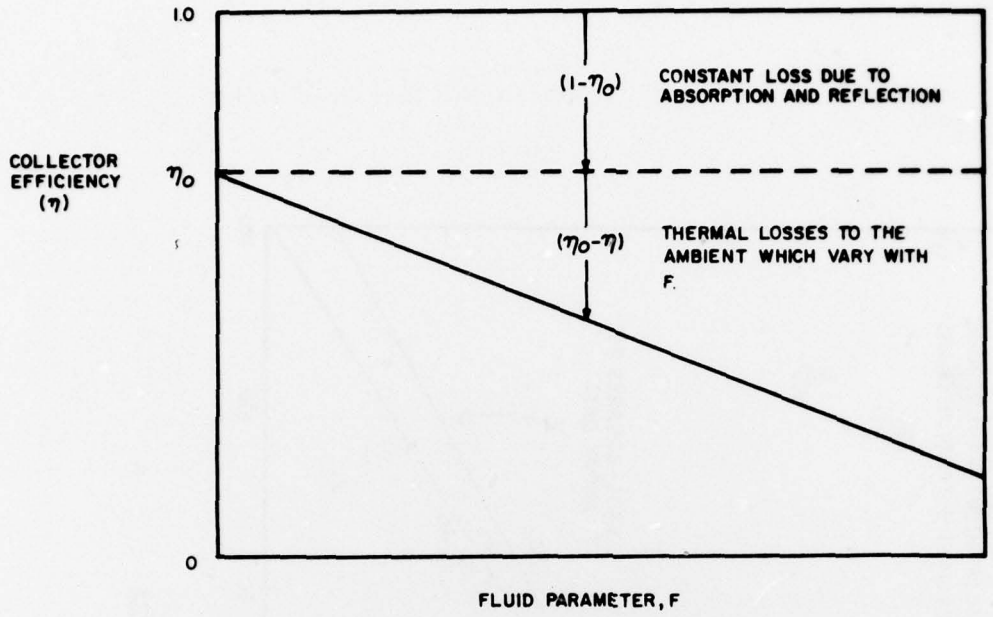

Figure 4. Sources of loss of collector efficiency.

tions are steady-state. The losses are separated into two types, as illustrated in Figure 4:

1. The constant loss, given by $1 - \eta_o$, which results from absorption in the glass cover and reflection from the absorber plate.

2. The loss to the ambient, given by $\eta_o - \eta$, which varies linearly with the fluid parameter, F.

To illustrate this feature of the plot, the single-collector test data of Figure 3 will be used. The intercept at F = 0 is .76; hence, the constant loss of collector efficiency due to glass absorption and plate reflection is 24 percent. The thermal losses to the ambient are then responsible for the remaining decrease in collector efficiency. $\eta_o - \eta$, as F is increased. For instance, at F = 65 (in SI units) the efficiency has dropped to 0.35, which indicates a decrease in efficiency of 41 percent due to the ambient losses for this value of F.

A least-squares-fit to a straight line was performed for each set of data shown in Figure 3. Table 12 lists values obtained by this procedure for the single collector and the array. Table 12 also provides the values obtained from a calculation employing the collector model and with the numerical specifications supplied by the collector manufacturer. The table indicates that there is generally good agreement between the two, although the manufacturer's specifications may be somewhat conservative.

It should be emphasized that scatter in the actual collector array performance is to be expected. The collector efficiency curve published by the manufacturer is performed on a single collector operating under ideal conditions. Data from the CERL collectors, however, reflect the performance of an entire array which is subject to ambient conditions.

Table 12

Collector Performance

Source of Data	Intercept η_o	Slope (10^{-3} $\frac{kW/m^2}{^oC}$)	U_{eff} $\frac{Btu}{sq\ ft\text{-}hr\text{-}^oF}$
1977-78 data for array	0.74	-5.6	0.38
Single coll. test data	0.78	-6.4	0.43
Calculated from specs.*	0.83	-5.1	0.34

*Specifications supplied by manufacturer: solar transmittance of glass, 0.92; absorptivity of absorber plate coating, 0.90; insulation behind absorber, R = 10.4; effective absorber area, 18.56 sq ft (1.68m^2); outside dimensions, 36 in. wide x 84 in. long x 4 in. thick (.914 x 2.134 x .102 m).

6 RESULTS

Overall Performance of the Solar System

Values for the daily average heat transfer between the major system components were obtained for the winter months of 1977-78. Representative values of these quantities, expressed per unit collector area are:

Heat output of collector array	0.85 kWh/m^2
Heat delivered to storage tank	0.79 kWh/m^2
Useful heat delivered to coil	0.70 kWh/m^2
	(Table 5)

Representative values of these quantities, expressed as a percentage of the incident solar energy, are:

Heat output of collector array	27 percent
Heat delivered to storage tank	26 percent
Useful heat delivered to coil	23 percent
	(Table 7)

Performance of the Solar System Components

The use of the heat exchanger in the collector loop was found to produce a loss of approximately 6 percent of the heat output of the collector array and to decrease the collector efficiency by approximately 2 percent.

The pumps used to collect and store the solar energy were found to deliver approximately 9 units of energy to the tank for each unit of electrical energy consumed.

Storage tank losses were calculated to be approximately 15 percent of the energy delivered to the tank. The relatively large size of this loss was attributed to the high tank volume to collector area ratio [.38m^3 /m^2 (9 gal/sq ft)].

The need for a distributed tank temperature sensor and precise energy measurements in the experimental determination of storage losses was established.

The effect of the inclination of the collectors was found to range from an average increase of 15 percent (in January) to an average decrease of 15 percent (in May) in the amount of solar energy incident on the collectors.

The performance of the collectors was investigated by using a procedure consistent with the one used by the National Bureau of Standards. Data analysis that was based on a simple model revealed that absorption in the glass cover and reflection from the absorber plate produced a fixed loss of 25 percent of the incident solar energy. Thermal losses to the ambient air, which increase linearly with the fluid parameter, were responsible for the remaining loss of collector efficiency, and were typically approximately 40 percent.

These research results indicate that the collector array is by far the most inefficient component in the system for transforming incident solar energy into useful heat. While not directly scalable to commercial-sized systems, the losses presented here may be considered typical for the preliminary design of a solar energy system which uses flat-plate collectors.

APPENDIX: INSTRUMENTATION SYSTEM

Introduction

To obtain the data necessary for evaluating the performance of the solar energy system, a data collection system capable of continuously measuring and recording the quantities listed in Tables 1 and 2 was required. Analog voltages corresponding to the instantaneous values of the temperatures, flow rates, and powers listed in Table 1 were produced by conventional sensors and signal-conditioning equipment. To obtain the products and integrals described in Table 2, these analog voltages were fed into electronic multipliers and/or integrators. Both these analog voltages and the outputs of the multipliers and integrators were measured each hour by a 40-channel data acquisition system and stored on a digital magnetic tape with a recording unit.

The following paragraphs describe the individual components of the instrumentation system.

Data Acquisition System

The data acquisition system employed was the Model D2020 manufactured by Esterline Angus Corporation. The unit contains a 3½ digit voltmeter (with full-scale ranges of 0.1, 1, and 1.0 volts) and a multiplexer with the capability of measuring up to 40 channels. The internal clock provided with the unit initiated the data-logging sequence each hour. The time indicated by the clock and an identification number controlled by switches mounted on the front panel (which was set to the Julian date for that day) were recorded immediately before logging the data. After the data-logging sequence was terminated, the unit provided a signal which reset the electronic integrators to zero.

Tape Recording System

The output of the data acquisition system was connected to a Model 815 tape recorder manufactured by Techtran Industries, Inc. This unit automatically recorded the data logged each hour by the data acquisition system on magnetic tape. Digital cassette tapes, having a storage capacity of approximately 9 days of data, also manufactured by Techtran Industries, were used in the tape recorder.

Electronic Multipliers and Integrators

The electronic multipliers were constructed, using integrated circuits and a standard power supply. The product of each pair of analog voltages was obtained by a single integrated circuit—the multi-function converter Model 4301 manufactured by Burr-Brown Research Corp. The manufacturer specified an accuracy of ±.25 percent of full-scale output.

The electronic integrators manufactured by Easterline Angus Corp. were purchased as part of the Model D2020 data acquisition system. Specifications supplied by the manufacturer indicate that the accuracy of the integrators is ±1 percent of full scale for an integration time of 1 hour.

Percent Solar Measurement

Figure A1 illustrates the novel method used to measure the fraction of the heating load supplied by the solar system (or percent solar). The arrows on the figure show the direction of signal flow through the circuits. By using an electronic multiplier with inputs from the flow and temperature circuitry associated with the coil, an electronic signal proportional to the instantaneous power being delivered to the coil was obtained. This "power" signal was connected directly to the input of one integrator to obtain the total heat delivered to the coil (i.e., the load). The "power" signal was also routed to a pair of solid-state switches connected to the input of a second integrator. The switches controlled the input of the second integrator in accordance with a control signal from the auxiliary heater. The relationship between the positions of the switches and the control signal was as follows:

1. When the control signal indicated that the auxiliary heater was "on," the switches connected the input of the second integrator to the circuit ground. This switch position is shown by the solid lines in the figure.

2. When the control signal indicated that the auxiliary heater was "off," the switches routed the "power" signal to the input of the second integrator. This switch position is shown by the dashed lines in the figure.

By using this scheme, the output of the second integrator was made to correspond to the useful heat delivered to the heating coil from the solar system (i.e., Q_{used}).

Since the power delivered to the coil from both sources was measured with the same sensors and circuitry, many of the equipment errors cancel when the percent solar is calculated from the ratio $Q_{used}/Load$.

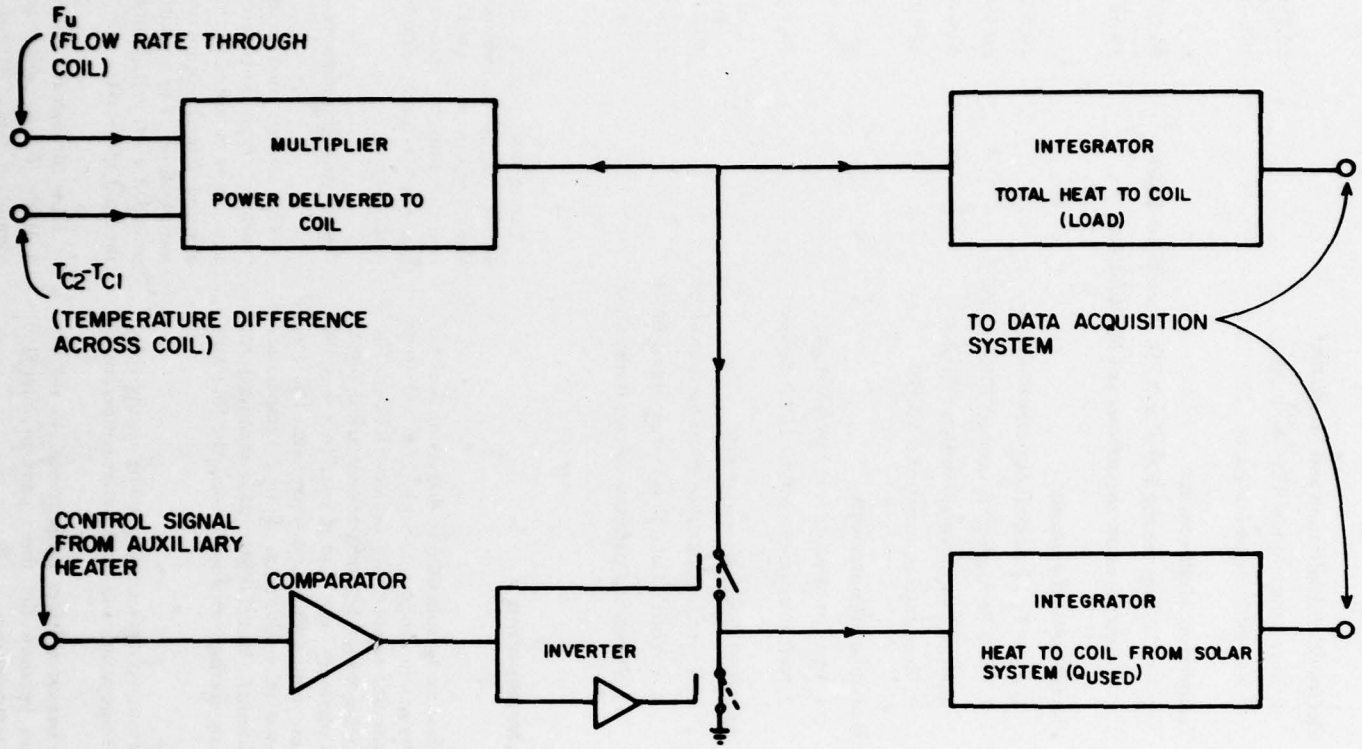

Figure A1. Sketch illustrating percent solar measurement.

Table A1

Instrument Accuracy

Electronic Multiplication and Integration	
1. Burr-Brown Model 4301 Multiplier	±0.25% of full scale
2. Esterline Angus Integrator	±1% of full scale
Temperature Measurements	
1. Hy-Cal Engineering 500 ohm RTD, Model ESD-9025	±0.05°C
2. Weather Measure thermistors and Model SC601	±0.15°C
Flow Rate Measurements	
1. Flow Technology flowmeter FT-12	±0.5% of full scale
2. Flow Technology flowmeter PRC-401A	±0.5% of full scale
3. Mead Instruments flowmeter PT-200	±1% of full scale
4. Mead Instruments Model FX-70	±2% of full scale
Radiation Measurements	
1. Weather Measure R413 pyranometers	±5%
2. Neff Instruments Model 119 Amplifier	±0.1% of full scale
Electrical Power Measurements	
1. Scientific Columbus Watthour transducers	±0.25%
2. Scientific Columbus current transformer	±1%
3. Scientific Columbus voltage transformer	±1%

Temperature Measurements

The temperature sensors used to determine the heat transfer between the collector, tank, and coil were platinum resistance temperature devices (RTDs). The well-known relationship between the electrical resistance of the platinum wire and temperature was the basis for these temperature measurements. The sensors were used in conjunction with a Temperature Signal Conditioner (Model ESD-9025) manufactured by Hy-Cal Engineering, which provided the following outputs:

1. Six output voltages corresponding to the three inlet temperatures and three outlet temperatures.

2. Three output voltages proportional to the differences between the three pairs of inlet and outlet temperatures.

The manufacturer claimed an accuracy of greater than ±0.1°F (−17.5°C) for all measurements of this system.

Thermistor probes and instrumentation (Model SC601 Signal Conditioner) supplied by Weather Measure Corp. were used to measure the tank temperature and ambient temperature. The accuracy given for this temperature measurement system was ±0.15°C (0.27°F).

Flow Rate Measurements

The sensors used to measure flow rate were the "turbine" type flow-meters. The small turbine of the sensor was mounted in the fluid stream and rotated at a speed directly proportional to the velocity of the moving fluid. The circuitry supplied with the sensors provided a DC voltage output directly proportional to the fluid's flow rate.

Flow through the collector loop was measured with a Model FT-12 sensor and Model PRC-401A instrumentation manufactured by Flow Technology, Inc. The sensor accuracy and instrumentation accuracy were each specified to be ±0.5 percent of the full-scale output.

The other two flow rates were measured with Model PT-200 sensors and Model FX-70 circuitry manufactured by Mead Instruments, Inc. The accuracy of the Model PT-200 was given as ±1%.

Radiation Measurements

The sensors used to measure the incident solar radiation were Model R413 Star Pyranometers purchased from Weather Measure Corp. The sensors contain 12 copper segments, painted alternately black and white, mounted beneath a glass dome. The incident solar radiation produced a temperature difference between the black and white segments which was converted to a voltage output by a thermopile consisting of 72 thermocouple junctions. The output voltages of the pyranometers were amplified with Model 119 amplifiers manufactured by Neff Instrument Corp. An accuracy of ±5 percent was estimated by directly comparing the outputs of the two pyranometers mounted in the same plane.

Electrical Power Measurements

The electrical power consumption of the pumps used to collect and store the solar energy was measured with standard watthour transducers in conjunction with current and potential transformers. The units were purchased from Scientific Columbus. The accuracy of the transducer was given as ±0.25 percent, whereas the transformers were listed as having an accuracy of ±1 percent.

Instrument Accuracy

Table A1 lists the accuracy of the instrumentation described above.

CERL DISTRIBUTION

Chief of Engineers
ATTN: DAEN-ASI-L (2)
ATTN: DAEN-MPE-S
ATTN: DAEN-MPE-E/S. Hiratsuka
Dept of the Army
WASH DC 20314

All Engineer Districts
ATTN: Chief, Engr Dist

Facilities Engineers listed
in PAM 210-1

Defense Documentation Center
ATTN: DDA (12)
Cameron Station
Alexandria, VA 22314

Joncich, David M
The performance of an experimental solar heating system / by D. M. Joncich, D. J. Leverenz, D. L. Johnson. -- Champaign, IL : Construction Engineering Research Laboratory ; Springfield, VA : available from NTIS, 1979.
23 p. ; 27 cm. (Interim report ; E-144)

1. Solar heating. I. Leverenz, Donald James. II. Johnson, David L. III. Title. IV. Series: U.S. Construction Engineering Research Laboratory. Interim report ; E-144.